

Methane paradox in tropical lakes? Sedimentary fluxes rather than pelagic production in oxic conditions sustain methanotrophy and emissions to the atmosphere

5 Cédric Morana^{1,2*}, Steven Bouillon¹, Vimac Nolla-Ardèvol¹, Fleur A.E. Roland², William Okello³, Jean-Pierre Descy², Angela Nankabirwa³, Erina Nabafu³, Dirk Springael¹, Alberto V. Borges².

¹Department of Earth & Environmental Sciences, KU Leuven, Belgium

²Chemical Oceanography Unit, Université de Liège, Belgium

³Limnology Unit, National Fisheries Resources Research Institute, Uganda

10 *Correspondence to:* Cédric Morana (Cedric.Morana@kuleuven.be)

Abstract. Despite growing evidence that methane (CH₄) formation could also occur in well-oxygenated surface freshwaters, its significance at the ecosystem scale is uncertain. Empirical models based on data gathered at high latitude predict that the contribution of oxic CH₄ increases with lake size and should represent the majority of CH₄ emissions in large lakes. However, such predictive models could not directly apply to tropical lakes which differ from their temperate counterparts in some
15 fundamental characteristics, such as year-round elevated water temperature. We conducted stable isotope tracer experiments which revealed that oxic CH₄ production is closely related to phytoplankton metabolism, and is a common feature in five contrasting African lakes. Nevertheless, methanotrophic activity in surface waters and CH₄ emissions to the atmosphere were predominantly fuelled by CH₄ generated in sediments and physically transported to the surface. Indeed, CH₄ bubble dissolution flux and diffusive benthic CH₄ flux were several orders of magnitude higher than CH₄ production in surface waters. Microbial
20 CH₄ consumption dramatically decreased with increasing sunlight intensity, suggesting that the freshwater “CH₄ paradox” might be also partly explained by photo-inhibition of CH₄ oxidizers in the illuminated zone. Sunlight appeared as an overlooked but important factor determining the CH₄ dynamics in surface waters, directly affecting its production by photoautotrophs and consumption by methanotrophs.

1. Introduction

25 Emissions from inland waters are an important component of the global CH₄ budget (Bastviken et al. 2011), in particular from tropical latitudes (Borges et al. 2015). While progress has been made in evaluating the CH₄ emission rates, much less attention has been given to the underlying microbial production (methanogenesis) and loss (methane oxidation) processes. It is generally assumed that CH₄ in lakes originates from the degradation of organic matter in anoxic sediments. Because most methanogens are considered to be strict anaerobes and net vertical diffusion of CH₄ from anoxic bottom waters is often negligible (Bastviken
30 et al. 2003), physical processes of CH₄ transport from shallow sediments are usually invoked to explain patterns of local CH₄ concentration maximum in surface waters (Encinas-Fernandez et al. 2016, Peeters et al. 2019, Martinez-Cruz et al. 2020). Indeed, CH₄-rich pore water is regularly released from littoral sediment into the water column during resuspension events associated with surface waves (Hofmann et al. 2010).

The view that CH₄ is formed under strictly anaerobic conditions has been challenged by several recent studies which proposed
35 that acetoclastic methanogens directly attached to phytoplankton cells are involved in epilimnetic CH₄ production (Grossart et al. 2011, Bogard et al. 2014), and are responsible of distinct near-surface peaks of CH₄ concentration in certain thermally stratified, well-oxygenated waterbodies (Tang et al. 2016). It has also been showed that Cyanobacteria (Bizic et al. 2020) and widespread marine phytoplankton (Klitzsch et al. 2019) are able to release substantial amount of CH₄ during a culture study, and this CH₄ production mechanism might be linked to photosynthesis. From a model-based approach, epilimnetic CH₄
40 production was shown to sustain most of the CH₄ oxidation in 14 Canadian lakes (DeIsonthro et al. 2018), and would even

represent up to 90% of the CH₄ emitted from a temperate lake (Donis et al. 2017). Further, empirical models based on data gathered in boreal and temperate lakes predict that the contribution of oxic CH₄ increases with lake size (Gunthel et al. 2019) and should represent the majority of CH₄ emissions in lakes larger than 1 km². Still, aerobic CH₄ production has so far only been documented in temperate and boreal lakes so that such predictive models could not directly apply to tropical lakes which differ from their temperate counterparts in some fundamental characteristics, such as year-round elevated water temperature. Primary production, methanogenic and methanotrophic activities, and cyanobacterial dominance are potentially much higher in tropical lakes due to favorable temperature (Lewis 1987, Kosten et al. 2012). It has also been shown that CH₄ emissions are positively related to temperature at the ecosystem scale (Yvon-Durocher et al. 2014)

Here, we tested the hypothesis that phytoplankton metabolism could fuel CH₄ production in well-oxygenated waters in five contrasting tropical lakes in East Africa covering a wide range of size, depth, and productivity (L. Edward, L. George, L. Katinda, L. Nyamusingere and L. Kyambura). Phytoplankton activity could provide diverse substrates required for CH₄ production mediated by methanogenic Archaea, or alternatively CH₄ could be directly released by phytoplankton cells. Additionally, the significance of epilimnetic CH₄ production at the scale of the aquatic ecosystem was assessed by quantifying CH₄ release from sediments, CH₄ production and oxidation rates in the water column, and CH₄ diffusive and ebullitive emissions to the atmosphere.

2. Material and methods

2.1. Site description

The sampled lakes cover a wide range of size (<1 to 2300 km²), maximum depth (3-117 m), mixing regimes, phytoplankton biomass and primary productivity (Table S1). Oligotrophic L. Kyamwinda (-0.18054°N, 30.14625°E) and eutrophic L. Katinda (-0.21803°N, 30.10702°E) are stratified, small but deep tropical lakes located in Western Uganda. Neighboring L. Nyamusingere (-0.284364°N, 30.037635°E) is a small but shallow and polymictic eutrophic lake. L. George is a larger (250 km²), hypereutrophic, shallow lake located at the equator (-0.02273°N, 30.19724°E). A single outlet (Kazinga Channel) flows from L. George to the neighboring Lake Edward (-0.28971°N, 29.73327°E), a holomictic, mesotrophic large lake (2325 km²). Water samples from pelagic stations of L. Katinda (0.3km from shore, 14m deep), L. George (2 km from shore, 2.5m deep) and L. Edward (15 km from shore, 20m deep) were collected in April 2017 (rainy season) and January 2018 (dry season). Pelagic sites of L. Kyamwinda (0.5 km from shore, 40m deep) and L. Nyamusingere (0.2 km from shore, 3 m deep) were sampled only once, in April 2017 and January 2018, respectively.

2.2. Environmental setting of the study sites

Conductivity, temperature and dissolved oxygen concentration measurements were performed with a Yellow Spring Instrument EXO II multiparametric probe. Samples for particulate organic carbon (POC) concentration were collected on glass fiber filters (0.7 μm nominal pore size) and analyzed with an elemental analyzer coupled to an isotope ratio mass spectrometer (EA-IRMS) (Morana et al. 2015). Pigment concentrations were determined by high performance liquid chromatography (Descy et al. 2016) after filtration of water samples through glass fiber filters (0.7 μm nominal pore size).

Water samples for determination of dissolved CH₄ concentration were transferred with tubing from the Niskin bottle to 60 ml borosilicate serum bottles that were poisoned with 200μL of a saturated solution of HgCl₂, closed with a butyl stopper and sealed with an aluminum cap. The concentrations of dissolved CH₄ was measured with the headspace equilibration technique (20 ml headspace) using a gas chromatograph with flame ionization detection (GC-FID, SRI8610C).

Samples for δ¹³C-CH₄ determination were collected in 60 ml serum bottles following the same procedure than samples for CH₄ concentration determination. In the laboratory, δ¹³C-CH₄ was measured as described in Morana et al. (2015). Briefly, a 20ml helium headspace was created in the serum bottles, then samples were vigorously shaken and left to equilibrate

overnight. The sample gas was flushed out through a double-hole needle and purified of non-CH₄ volatile organic compounds in a liquid N₂ trap, CO₂ and H₂O were removed with a soda lime and a magnesium perchlorate traps, and the CH₄ was converted to CO₂ in an online combustion column similar to that in an elemental analyzer (EA). The resulting CO₂ was subsequently preconcentrated in a custom-built cryo-focussing device by immersion of a stainless-steel loop in liquid N₂, passed through a
85 micro-packed GC column (HayeSep Q 2 m, 0.75mm ID; Restek), and finally measured on a Thermo Scientific Delta V Advantage isotope ratio mass spectrometer (IRMS). CO₂ produced from certified reference standards for δ¹³C analysis (IAEA-CO1 and LSVEC) were used to calibrate δ¹³C-CH₄ data. Reproducibility of measurement estimated based on duplicate injection of a selection of samples was typically better than 0.5 ‰, or better than 0.2‰ when estimated based on multiple injection of standard gas.

90 2.3. Diffusive CH₄ flux calculation

Surface CH₄ concentrations were used to compute the diffusive air-water CH₄ fluxes (FCH₄) according to eq. (1):

$$FCH_4 = k \times \Delta CH_4 \quad (1)$$

95 Where k is the gas transfer velocity of CH₄ computed from wind speed (Cole & Caraco 1998) and the Schmidt number of CH₄ in freshwater (Wanninkhof 1992), and ΔCH₄ is the air-water gradient. Wind speed data were acquired with a Davis Instruments meteorological station located in Mweya peninsula (0.11°S 29.53°E).

2.4. CH₄ ebullition flux

CH₄ ebullition flux was investigated in L. Edward (at 20 m), George (at 2.5 m), and Nyamusingere (at 3 m) only, at
100 the same sampling sites where biogeochemical processes were measured. Bubble traps made with an inverted funnel (24 cm diameter) connected to a 60 ml syringe were deployed for a period between 24 h and 48 h at 0.5 m below the water surface (4 replicates). Measurements were performed at sites with water depth of 20 m, 2.5 m and 3 m for L. Edward, George and Nyamusingere, respectively. After measuring the gas volume collected within the trap during the sampling period, the gas bubbles were transferred in a tightly closed 12 ml Exetainer vial (Labco) for subsequent analysis of their CH₄ concentration.
105 Variability of the gas volume in the 4 replicates was less than 10%. We used the SiBu-GUI software (McGinnis et al. 2006, Greinert et al. 2009) to correct for gas exchange within the water column during the rise of bubbles and thus obtained the CH₄ ebullition and CH₄ bubble dissolution fluxes. Calculations were made following several scenarios: two extreme bubble-size scenarios considering a release of many small (3 mm diameter) bubbles or fewer large (10 mm) bubbles, and an intermediate scenario of release of 6 mm diameter bubbles. Delwiche & Hemond (2017) experimentally determined that a large majority
110 (~ 90%) of the bubbles released from lake sediments fall in this size interval.

2.5. Potential CH₄ flux across the sediment-water interface

The potential CH₄ flux across the sediment-water interface was determined from short-term intact core incubations in L. Edward, L. George and L. Nyamusingere only, at the same sampling sites where biogeochemical processes were measured. CH₄ flux was quantified from the change of CH₄ concentration in overlying waters at 5 different time steps, every
115 2 hours. Briefly, in every lake, 2 sediment cores (6 cm wide; ~ 30 cm sediment and 30 cm of water) were collected taking care to avoid disturbance at the sediment-water interface. Cores were kept in the dark until back in the laboratory, typically 6h later. Overlying water was carefully removed with a syringe taking care to avoid any disturbance of the sediments. It was replaced by bottom lake water which had been previously filtered through 0.2µm polycarbonate filters (GSWP, Millipore) in order to remove water column methanotrophs and degassed with helium during 20 minutes in order to remove background O₂ and
120 CH₄. and the filtered and degassed water was gently returned in the core tubes, on top of the sediments. Core tubes were tightly closed with a thick rubber stopper equipped with two sampling valves. A magnetic stirrer placed ~ 10 cm above the sediments

was allowed to rotate gently in order to homogenize the overlying water layer during the incubation. At each time step, 60 ml of overlying water was sampled by connecting a syringe to the first sampling valve while an equivalent volume of degassed water was allowed to flow through the second valve in order to avoid any pressure disequilibrium. Subsamples of overlying water were transferred into a two 20 ml serum bottles filled without headspace and poisoned with HgCl₂. Determination of the dissolved CH₄ concentration was performed with a GC-FID following the same procedure as described above. The removal of oxygen might have inhibited the biogeochemical activity of aerobic methanotrophs present at the sediment-water interface, hence we considered that the results gathered from this experiment are representative of a potential (maximal) CH₄ flux.

2.6. Primary production and N₂ fixation

Primary production and N₂ fixation rates were determined from dual stable isotope photosynthesis-irradiance experiments using NaH¹³CO₃ (Eurisotop) and dissolved ¹⁵N₂ (Eurisotop) as tracers for incorporation of dissolved inorganic carbon (DIC) and N₂ into the biomass. The ¹⁵N₂ tracer was added dissolved in water (Mohr et al. 2010). Incident light intensity was measured by a LI-190SB quantum sensor during day time during the entire duration of the sampling campaign. At each station a sample of surface waters (500 ml) was spiked with the tracers (final ¹⁵N atom excess ~5%). Three subsamples were preserved with HgCl₂ in 12-mL Exetainers vials (Labco) for the determination of the exact initial ¹³C-DIC and ¹⁵N-N₂ enrichment. The rest of the sample was divided into nine 50-ml polycarbonate flasks, filled without headspace. Eight flasks were placed into a floating incubation device providing a range of light intensity (from 0 to 80% of natural light) using neutral density filter screen (Lee Filters). The last one was immediately amended with neutral formaldehyde (0.5% final concentration) and served as killed control sample. Samples were incubated *in situ* during 2 hours around mid-day just below the surface at lake surface temperature. After incubation, biological activity was stopped by adding neutral formaldehyde into the flasks, and the nine samples were filtered on pre-combusted GF/F filters when back in the lab. Glass fiber filters were decarbonated with HCl fumes overnight, dried, and their δ¹³C-POC and δ¹⁵N-PN values were determined with an EA-IRMS (Thermo FlashHT – delta V Advantage). For the measurement of the initial ¹⁵N₂ enrichment, a 2-ml helium headspace was created, and after 12h equilibration, a fraction of the headspace was injected into the above-mentioned EA-IRMS equipped with a Cu column warmed at 640°C and a CO₂ trap. Initial enrichment of ¹³C-DIC was also measured.

Photosynthetic (P_i) (Hama et al. 1983) and N₂ fixation (N₂fix_i) (Montoya et al. 1996) rates in individual bottles were calculated, and corrected for any abiotic tracer incorporation by subtraction of the killed control value. For each experiment, the maximum photosynthetic and N₂ fixation rates (P_{max}, N₂fix_{max}) and the irradiance at the onset of light saturation (I_{k_PP}, I_{k_N2fix}) were determined by fitting P_i and N₂fix_i to the light intensity gradient provided by the incubator (I_i) using the equation (eq. 2) for photosynthesis activity (Vollenweider 1965) and (eq. 3) for N₂ fixation (Mugidde et al. 2003).

$$P_i = 2P_{max} \left[\frac{I_i/2I_{k_PP}}{1 + (I_i/2I_{k_PP})^2} \right] \quad (2)$$

$$N_2fix_i = 2N_2fix_{max} \left[\frac{I_i/2I_{k_N2fix}}{1 + (I_i/2I_{k_N2fix})^2} \right] \quad (3)$$

2.7. Determination of CH₄ oxidation rates.

CH₄ oxidation rates in surface waters (1m depth) were determined from the decrease of CH₄ concentrations measured during short (typically < 24h) time course experiments. Samples for CH₄ oxidation rate measurement were collected in 60 mL glass serum bottles filled directly from the Niskin bottle with tubing, left to overflow, and immediately closed with butyl stoppers previously boiled in milli-Q water, and sealed with aluminum caps. The first bottle was then poisoned with a saturated solution of HgCl₂ (100 μl) injected through the butyl stopper with a polypropylene syringe and a steel needle and corresponded to the initial CH₄ concentration at the beginning of the incubation (T₀).

The remaining bottles were incubated in the dark, at in situ (~26°C) temperature during ~12h or ~24h except in L. George and Nyamusingere where the incubation was shorter (~6h). At 4 different times step one bottle was poisoned with 100 μL of HgCl_2 and stored in the dark until measurement of the CH_4 concentrations with the above-mentioned GC-FID. CH_4 oxidation rates were calculated as a linear regression of CH_4 concentrations over time (r^2 generally better than 0.80) during the course of the incubation. O_2 consumption was followed in a parallel incubation of water samples in 60 mL biological oxygen demand bottles (Wheaton) to ensure the samples were incubated under oxic conditions during the full course of this short-term experiment.

170

2.8. Sunlight inhibitory effect on CH_4 oxidation

The influence of light intensity on methanotrophy was investigated in L. Edward (April 2017 and January 2018), L. Nyamusingere and L. George (January 2018) by means of a stable isotope ($^{13}\text{CH}_4$) labelling experiment. For each experiment, 12 serum bottles (60 mL) were filled with lake surface waters (1 m) as described above. All bottles were spiked with 100 μL of a solution of dissolved $^{13}\text{CH}_4$ (50 $\mu\text{mol L}^{-1}$ final concentration, 99% enrichment) added in excess. In L. Edward in January. Half of the bottles were amended with 3-(3,4-dichlorophenyl)-1,1-dimethylurea (DCMU, 0.5 mg L^{-1}) in order to inhibit photosynthesis (Bishop 1958) and investigate the hypothetical inhibitory effect of dissolved O_2 production by phytoplankton. Two bottles were poisoned immediately with pH-neutral formaldehyde (0.5% final concentration) and served as killed controls. The ten others were incubated during 24h at 26°C in a floating device providing 5 different light intensities (from 0 to 80% of natural light using neutral density filter screens (Lee Filters). For every bottle at the end of the incubation, one 12-mL vial (Labco Exetainer) was filled with the water sample and preserved with 50 μL HgCl_2 . The rest of the sample (~50 mL) was filtered on a precombusted GF/F filter for subsequent $\delta^{13}\text{C}$ -POC measurement.

$\delta^{13}\text{C}$ -DIC and $\delta^{13}\text{C}$ -POC were determined with an EA-IRMS following the method described in Gillikin & Bouillon (2007) and Morana et al. (2015), respectively. The methanotrophic bacterial production, defined at the CH_4 -derived ^{13}C incorporation rates into the POC pool was calculated as in eq. (4) (Morana et al. 2015):

185

$$MBP = \frac{POC_t \times (\%^{13}\text{C}POC_t / \%^{13}\text{C}POC_i)}{t \times (\%^{13}\text{C}CH_4 / \%^{13}\text{C}POC_i)} \quad (4)$$

Where POC_t is the concentration of POC after incubation, $\%^{13}\text{C-POC}_t$ and $\%^{13}\text{C-POC}_i$ are the final and initial percentage of ^{13}C in the POC, t is the incubation time and $\%^{13}\text{C-CH}_4$ is the percentage of ^{13}C in CH_4 after the inoculation of the bottles with the tracer. Similarly, the methanotrophic bacterial respiration rates, defined as the CH_4 -derived ^{13}C incorporation rates into the DIC pool, were calculated as in eq. (5):

190

$$MBR = \frac{DIC_t \times (\%^{13}\text{C}DIC_t / \%^{13}\text{C}DIC_i)}{t \times (\%^{13}\text{C}CH_4 / \%^{13}\text{C}DIC_i)} \quad (5)$$

195

Where DIC_t is the concentration of DIC after the incubation, $\%^{13}\text{C-DIC}_t$ and $\%^{13}\text{C-DIC}_i$ are the final and initial percentage of ^{13}C in DIC and $\%^{13}\text{C-CH}_4$ is the percentage of ^{13}C in CH_4 after the inoculation of the bottles with the tracer.

Potential CH_4 oxidation rates (MOX) were calculated as the sum of MBP and MBR rates. The fraction (%) of MOX inhibited by light was calculated at every light intensity as (eq.6):

200

$$MOX_{inhibition}(\%) = (1 - MOX_i / MOX_{dark}) \times 100 \quad (6)$$

Where MOX_i is the potential CH_4 oxidation for a given light treatment and MOX_{dark} is the potential CH_4 oxidation in the dark.

2.9. Determination of pelagic CH₄ production rates.

205 Time course ¹³C tracer experiments were carried out in well oxygenated surface waters at every sampling site. Measurement of the isotopic enrichment of the CH₄ during this experiment allowed to estimate production rates of CH₄ issued from 3 different precursors: ¹³C-DIC (NaH¹³CO₃), ¹³C_(1,2)-acetate and ¹³C_{methyl}-methionine. Serum bottles (60 ml) were spiked with 1 ml of ¹³C tracer solution, or with an equivalent volume of distilled water for the control treatment. NaH¹³CO₃ was added in the bottles at a tracer level (less than 5% of ambient HCO₃⁻ concentration) while ¹³C_(1,2)-acetate and ¹³C_{methyl}-methionine
210 were added largely in excess (>99% of ambient concentration). Therefore, we assume the CH₄ production rates measured from ¹³C-DIC could be representative of in-situ rates, but the production rates measured from ¹³C-acetate and ¹³C-methionine should instead be viewed as potential rates. The exact amount of ¹³C-DIC added in the bottles was determined filling a borosilicate 12 ml exetainer vials preserved and analysed for δ¹³C-DIC as described above.

The control bottles and the bottles amended with the different ¹³C tracer were incubated under constant temperature
215 conditions (26°C) following three different treatments : (1) one third were incubated under constant light (PAR of ~ 200 μmol photon m⁻² s⁻¹), (2) another third were incubated under the same light intensities conditions but were first amended with DCMU (0.5 mg L⁻¹ ; final concentration), an inhibitor of photosynthesis, (3) and the last third were incubated in the dark.

At each time step (typically every 6-12h, 5-time steps), the biological activity was stopped by adding 100 μL of a saturation solution of HgCl₂. Bottles were kept in the dark until CH₄ concentration measurement and δ¹³C-CH₄ determination
220 as described above. O₂ consumption was followed in a parallel incubation of water samples in 60 mL biological oxygen demand bottles (Wheaton) to ensure the samples were incubated under oxic conditions during the full course of the experiment.

The term CH₄_{prod} (nmol L⁻¹ h⁻¹) defined as the amount of CH₄ produced from a specific tracer during a time interval t (h), was calculated following this equation (eq. 7) derived from Hama et al. (1983):

$$225 \quad CH_{4_prod} = \frac{CH_{4_t} \times (\%^{13}CCH_{4_t} / \%^{13}CCH_{4_i})}{t \times (\%^{13}C_{tracer} / \%^{13}CCH_{4_i})} \quad (7)$$

Where CH₄_t and %¹³CCH₄_t, represent the CH₄ concentration (nmol L⁻¹) and the %¹³C atom of the CH₄ pool at a given time step, respectively. %¹³CCH₄_i represent the %¹³C atom of the pool of CH₄ at the beginning of the experiment. %¹³C_{tracer} represent the %¹³C atom of the isotopically enriched pool of the precursor molecule tested (NaHCO₃, methionine
230 or acetate, depending of the treatment). %¹³C-tracer was assumed constant during the full course of the incubation given the high concentration of ambient DIC in the sampled lakes (~ 2 mmol L⁻¹ in L. George, > 6 mmol L⁻¹ in the other lakes) and that acetate and methionine were spiked in large excess (>99%).

2.10. DNA extraction

Surface water sample for DNA analysis (between 1 L and 0.15 L, depending on the biomass) were first filtered
235 through 5.0 μm pore size polycarbonate filters (Millipore). The eluent was then subsequently filtered through 0.2 μm pore size polycarbonate filters (Millipore) to retain free living prokaryotes. Filters were stored frozen (-20°C) immersed in a lysis buffer until processing in the laboratory. Total DNA was extracted from the 0.2 μm and 5.0 μm 47 mm filters using DNeasy PowerWater kit (Qiagen) following the manufacturer's instructions. Quality and quantity of the extracted DNA were estimated using the NanoDrop ND-1000 spectrophotometer (ThermoFisher) and the Qubit 3.0 fluorometer (Life technology). Extracted
240 DNA was stored at -20 °C until further use.

2.11. Quantification of *mcrA* via qPCR

Quantification of *mcrA* gene copies was performed by quantitative PCR (qPCR) on the total extracted DNA. The used primer pair consisted of forward primer *qmcrA-F* 5'-TTCGGTGGATCDCARAGRGC-3' and *qmcrA-R* 5'-GBARGTCGAWCCGTAGAATCC-3' (Denman et al. 2007). The reaction mixture contained 3 μL of total community

245 DNA extract, 7.5 μL Absolute qPCR SYBR Green Mix (ThermoFisher, Cat. AB1158B), 0.3 μL of 10 μM forward primer *mcrF*, 0.3 μL of 10 μM reverse primer *mcrR*, 1.5 μL of a 1% w/v Bovine Serum Albumin solution (Amersham Bioscience) and 2.4 μL of Nuclease/DNA-free water. The qPCR was performed in a Rotorgene 3000 (Corbett Research) using the following conditions: 95 $^{\circ}\text{C}$ (15 min) followed by 40 cycles of 20 s at 95 $^{\circ}\text{C}$, 20 s at 58 $^{\circ}\text{C}$, 20 s at 72 $^{\circ}\text{C}$ and a final extension step of 5 s at 80 $^{\circ}\text{C}$. Standard curves were prepared from serial dilutions of a prequantified *mcrA* PCR fragment amplified
250 using primers *mcrF* and *mcrR* from a plasmid extract carrying the complete *mcrA* gene using concentrations ranging from 1×10^2 to 1×10^8 copies μL^{-1} . Samples were analyzed in triplicates.

2.12. 16S rRNA gene amplicon sequencing

Sequencing of the 16S rRNA gene was done on the total extracted DNA to assess community composition. 16S rRNA gene sequencing was done with the Illumina MiSeq v3 Chemistry following the “16S Metagenomic Sequencing Library
255 Preparation” protocol with the following universal 16S rRNA gene primers targeting the V4 region, forward UniF/A519F-(S-D-Arch-0519-a-S-15) 5'-CAGCMGCCGCGGTAA-3' and reverse UniR/802R-(S-D-Bact-0785-b-A-18) 5'-TACNVGGGTATCTAATCC-3' (Klindworth et al. 2013). Sequenced read quality was checked using FastQC v0.11 (<https://www.bioinformatics.babraham.ac.uk/projects/fastqc/>). Short reads were trimmed to 250 bp with FastX Toolkit v0.0.13 (http://hannonlab.cshl.edu/fastx_toolkit/) in order to remove trailing Ns and low quality bases. Operational Taxonomical Units
260 (OTU) for each analyzed sample were obtained from the quality trimmed reads using mothur v1.39.5 (Kozich et al. 2013) and following the online MiSeq SOP (https://mothur.org/wiki/MiSeq_SOP - accessed April 2018) using the Silva v128 16S rRNA database with the following parameters: *maxambig* = 0 bp; *maxlength* = 300 bp; *maxhomop* = 8; and classify OTUs to 97% identity. Generated OTU table was used to calculate relative abundances of each OTU per sample.

3. Results

265 3.1. Environmental settings

The sampled lakes cover a wide range of size (<1 to 2300 km^2), maximum depth (3-117 m), mixing regimes, phytoplankton biomass and primary productivity (Table S1, Fig. S1). Phytoplankton biomass (Chlorophyll-a from 3.6 $\mu\text{g L}^{-1}$ to 190.2 $\mu\text{g L}^{-1}$) was dominated by Cyanobacteria (>95%) in the most productive lakes, while Diatoms (<20%) and Chrysophytes (<40%) also contributed in the less productive ones (Fig. S2). Maximum potential photosynthetic activity (P_{max})
270 varied from 1.5 $\mu\text{mol C L}^{-1} \text{h}^{-1}$ in L. Edward to 199.0 $\mu\text{mol C L}^{-1} \text{h}^{-1}$ in L. George and was linearly related to chlorophyll a concentration. Light-dependent N_2 fixation was detected in every lake with the exception of L. Kyamwinda. No significant N_2 fixation rates were measured in the dark. Maximum potential N_2 fixation rates ($\text{N}_2\text{fix}_{max}$) ranged between 1 $\text{nmol L}^{-1} \text{h}^{-1}$ and 128 $\text{nmol L}^{-1} \text{h}^{-1}$ and were positively related to P_{max} (Fig. S1).

We detected and quantified the abundance of the archaeal alpha subunit of methyl-coenzyme M reductase gene
275 (*mcrA*), a proxy for methanogens, in the surface waters of each lake. *mcrA* gene copy abundance (*mcrA* copy ng DNA^{-1}) ranged between 319 ± 41 (L. Edward) and 7537 ± 476 (L. Katinda) in the fraction of seston < 5 μm , and between 541 ± 19 (L. Edward) and 7968 ± 167 (L. Katinda) in the fraction of seston > 5 μm (Fig. S3). Illumina 16S rRNA gene amplicon sequencing indicated that methanogens accounted for a small fraction of the prokaryotic community in the surface waters of L. Edward (0.01 %), L. Kyamwinda (0.03 %) and L. Nyamunsingere (0.08 %). They represented a substantially higher fraction of the community
280 in L. Katinda (0.38%) and L. George (0.57 %) (Fig. S4). In all lakes, hydrogenotrophic (*Methanomicrobiales* and *Methanobacteriales*) were always more abundant than acetoclastic (*Methanosarcinales*) microorganisms, representing at least 65% of the methanogens (up to 95% in L. Katinda, Fig. S4).

3.2. Water column CH_4 concentration and $\delta^{13}\text{C}-\text{CH}_4$ patterns

Surface waters were super-saturated in CH_4 in all lakes, with surface concentrations (at 1 m) ranging between 78 and
285 652 nmol L^{-1} (atmospheric equilibrium $\sim 2 \text{ nmol L}^{-1}$). Diffusive CH_4 emissions varied between 0.05 $\text{mmol m}^{-2} \text{d}^{-1}$ (L. Edward)

and 0.40 mmol m⁻² d⁻¹ (L. Katinda). The benthic CH₄ flux across the sediment-water interface was elevated in comparison with the diffusive CH₄ emissions in the three lakes where it was measured: L. Edward (0.96 mmol m⁻² d⁻¹), L. George (9 mmol m⁻² d⁻¹) and L. Nyamusingere (5 mmol m⁻² d⁻¹). CH₄ ebullition was the dominant pathway of CH₄ evasion to the atmosphere in the 3 lakes (L. Edward, L. George, L. Nyamusingere) where ebullitive fluxes were investigated. Ebullitive flux in L. Edward ranged between 0.16 and 0.24 mmol m⁻² d⁻¹ depending of the bubble-size scenario considered (see material & methods), being at least 4 times higher than the diffusive CH₄ flux. This discrepancy was even larger in the shallower L. George (13.26-13.9 mmol m⁻² d⁻¹) and L. Nyamusingere (19.03-19.09 mmol m⁻² d⁻¹) where CH₄ ebullition appeared ~100 and ~50 times higher than diffusive CH₄ emissions. During the ascent of CH₄ bubbles to the surface, gas exchange occurs, and we estimated that, depending of the CH₄ bubble size considered, between 0.04 and 0.21 mmol CH₄ m⁻² d⁻¹ dissolved in the water column of L. Edward during bubble ascent. This bubble dissolution flux ranged between 0.70 – 3.30 mmol m⁻² d⁻¹ and 1.21 – 5.55 mmol m⁻² d⁻¹ in L. George and L. Nyamusingere, respectively.

Vertical patterns of CH₄ and stable carbon isotope composition of CH₄ (δ¹³C-CH₄) were variable among the different lakes. In L. Kyamwinda and Katinda, higher CH₄ concentrations and lower δ¹³C-CH₄ values were observed in the well-oxygenated epilimnion compared to the metalimnion showing a source of relatively ¹³C-depleted CH₄ to the epilimnetic CH₄ pool (Fig. 1). The CH₄ concentrations and δ¹³C-CH₄ were homogeneous in the water column of L. Edward that is much larger than the other studied lakes (2300 km², Table S1) and characterized by a higher wind exposure and a substantially weaker thermal stratification (Fig. 1). However, a clear horizontal gradient in CH₄ concentration and δ¹³C-CH₄ occurred between the littoral and pelagic zones (Fig. S5). Vertical gradients were also observed at much smaller scale in the near sub-surface (top 0.3 m) in the shallow and entirely well oxygenated L. George and L. Nyamusingere (Fig. 2). In both lakes CH₄ concentrations were relatively modest in the hypolimnion (< 50 nmol L⁻¹) but increased abruptly in the thermal gradient (0.3 m interval) to reach a surface maximum > 240 nmol L⁻¹ (Fig. 2). δ¹³C-CH₄ mirrored this pattern with significantly lower values in surface than at the bottom of the water column indicating that a source of relatively ¹³C-depleted CH₄ contributed to the higher epilimnetic CH₄.

CH₄.3.3. Occurrence of microbial CH₄ production in surface waters under oxic conditions

Despite the prevalence of oxic conditions, ¹³C-labelling experiments revealed that CH₄ was produced in surface waters of each lake with the exception of L. Kyamwinda (Fig. 3). The kinetic of incorporation of NaH¹³CO₃ into the CH₄ pool revealed that a substantially higher amount of CH₄ was produced from dissolved inorganic carbon (DIC) in illuminated waters, and this mechanism of CH₄ formation appears to be related to photosynthesis, as none or only modest quantities of CH₄ were produced from ¹³C-labelled DIC under darkness or when photosynthesis was inhibited by DCMU (Figs. 3a and S6). Furthermore, CH₄ production from DIC appeared strongly correlated (r² = 0.91) to the photosynthetic activity (Fig. 4a) and N₂ fixation rates (Fig 4b), supporting the view that CH₄ formation in oxic waters was directly linked to phytoplankton metabolism (Bizic et al. 2020).

Aside from DIC, an appreciable amount of CH₄ was generated in all lakes from the sulfur bonded methyl group of methionine when bottles were incubated under light, irrespective of the addition of DCMU (Fig. 3b and S6), that were approximately 4 times higher than in the dark. In addition, a positive relationship between CH₄ production from methionine in the light and the photosynthetic activity was found (Fig. 4c).

¹³C-labelled acetate, the substrate of acetoclastic methanogenesis, supported the production of CH₄ in all lakes with the exception of L. Kyamwinda, but at much lower rates compared to light-dependent CH₄ production from DIC (50 times lower, n=7) or methionine (10 times lower, n=4) (Fig. 3c and S6). δ¹³C analysis of the DIC in the bottles spiked with ¹³C-labelled acetate showed that the acetate was mineralized at rates of 5-6 orders of magnitude higher than acetoclastic methanogenesis so that added acetate appeared to be used almost exclusively by heterotrophic micro-organisms other than methanogens. Pattern of acetate-derived production of CH₄ were similar in light and dark treatments (Figs. 3c and S6) and this mode of CH₄ production appeared unrelated to phytoplankton activity (Fig. 4d).

3.4. Microbial methane oxidation

Net CH₄ oxidation was detected in all 5 investigated lakes ranging from 11 to 5212 nmol L⁻¹ d⁻¹ (Fig. 5), and was by far the largest loss term of dissolved CH₄ at ecosystem scale (8 to 46 times higher than the diffusive emission to the atmosphere). Surface water CH₄ turnover times were particularly short in the shallow and eutrophic L. George (2h) and L. Nyamusingere (3h) and slightly longer in the deeper and less productive L. Katinda (11h), L. Kyamwinda (77h) and L. Edward (100h). In all studied lakes, the volumetric CH₄ oxidation rates were always much higher than the volumetric CH₄ production we measured during the stable isotope tracer experiments, regardless of the CH₄ precursors tested. Pelagic CH₄ production rates represented 8.5%, 2.6%, 0.2% and 0.1% of CH₄ oxidation rates, in L. Edward, George, Katinda and Nyamusingere, respectively.

The influence of light on methanotrophy was investigated in the deep L. Edward, and shallow L. George and L. Nyamusingere, revealing that CH₄ oxidation rates decreased dramatically with increasing light intensity (Fig. 5). For instance, when exposed to full sunlight intensity, methanotrophs consumed only 42% (L. Edward), 54% (L. Nyamusingere) or 74% (L. George) of the CH₄ they were able to oxidize in the dark. The magnitude of this sunlight-induced inhibition decreased substantially with decreasing sunlight intensities (Fig. 5). In L. Edward (April 2017) sunlight inhibition of methanotrophy followed the same pattern of lower rates at high sunlight intensities in the bottles where O₂ production (via photosynthesis) was stopped by DCMU addition.

4. Discussion

4.1. Mechanisms of CH₄ production under aerobic conditions

The results from the stable isotope labelling experiment highlight that only a minimal fraction of the CH₄ produced under aerobic conditions originated from acetate in contrast with several earlier studies (Bogard et al. 2014, Donis et al. 2017) which proposed, based on the apparent fractionation factor of δ¹³C-CH₄, that acetoclastic methanogenesis linked to phytoplankton production of organic matter would be the dominant biochemical pathway of pelagic CH₄ production in oxic freshwaters. Instead, our results support the study of Bizic et al. (2020) and suggest that epilimnetic CH₄ production in well-oxygenated conditions was related to DIC fixation by photosynthesis (Fig. 3), and correlated to primary production (Fig. 4a) and N₂ fixation (Fig 4b). When normalized to POC concentrations, the average DIC-derived CH₄ production rates (0.08 ± 0.05 nmol mmol_{POC}⁻¹ h⁻¹ n = 7) was remarkably similar to the CH₄ production rates recently reported in Cyanobacteria cultures (0.04 ± 0.02 nmol mmol_{POC}⁻¹ h⁻¹) grown at 30°C, among which the freshwater *Microcystis aeruginosa* (Bizic et al. 2020), the dominant Cyanobacterium species in the tropical lakes investigated in our study (see Fig S2). These CH₄ production rates are 2 orders of magnitude higher than rates reported in an axenic culture of the eukaryote *Emiliania huxleyi* (0.19 ± 0.07 pmol mmol_{POC}⁻¹ d⁻¹) (Lenhart et al. 2016), but they are 4 orders of magnitude lower than typical anoxic CH₄ production rates by methanogenic Archaea (Mountford & Asher 1979). Although it seems improbable that ¹³C-DIC acted as a direct precursor molecule for the CH₄ released by phytoplankton (Lenhart et al. 2016, Klintzsch et al. 2019) ¹³C-DIC could have been taken up by phytoplankton cells and then used as a C source for the synthesis of many different organic molecules that may serve as the actual CH₄ precursors. Indeed, healthy phytoplankton cells actively release a variety of low molecular weight molecules which are generally highly labile and rapidly consumed (Baines & Pace 1991, Morana et al. 2014). Phytoplankton metabolism could have fuelled CH₄ production pathways, at least partially, excreting substrates involved in CH₄ production via biochemical processes such as demethylation of a variety of organic molecules like methionine, one of the S-bonded methylated amino acids (Lenhart et al. 2016), trimethylamine (Bizic et al 2018), or methylphosphonate (Yao et al. 2016).

While the source of methylphosphonate in freshwaters is obscure and its actual natural abundance remains to be determined, dissolved free amino acids would represent up to 4% of the DOC produced by phytoplankton and are rapidly consumed by heterotrophic bacteria (Sarmiento et al. 2013). Our incubations indeed demonstrated that the methyl group of

methionine was a potential precursor of CH₄ in all lakes investigated, in line with recent findings showing that *Emiliana*
370 *huxleyi* could act as a direct source of CH₄ in oxic conditions using methionine as precursor, without involvement of any other
micro-organisms (Lenhart et al. 2016). We found that CH₄ production from methionine was clearly stimulated under light,
even when photosynthetic activity was inhibited by DCMU, while little CH₄ from methionine was produced in darkness (Fig.
3b). DCMU notably prevents reduction of plastoquinone at photosystem II and generates singlet oxygen (Petrillo et al. 2014).
The mechanism of CH₄ production from methionine is still unclear, but its residue in proteins is particularly sensitive to
375 oxidation to methionine sulfoxide by radical oxygen species (ROS) (Levine et al. 1996) so that methionine would act as an
effective ROS scavenger and play important protective roles under photooxidative stress conditions, as shown in vascular
plants (Bruhn et al. 2012). The side chain of methionine sulfoxide is identical to dimethyl sulfoxide which is known to react
with hydroxyl radicals (OH) to form CH₄ (Repine et al. 1979). Besides its photoprotective role for phytoplankton, methionine
could also be catabolized by a wide variety of microorganisms to methanethiol, which could in turn be transformed to CH₄ as
380 shown in Arctic Ocean surface waters (Damm et al. 2010). Nevertheless, occurrence of this latter mechanism in the tropical
lakes investigated seems unlikely as this mode of CH₄ production would be expected to be insensitive to light irradiance and
no CH₄ was produced from methionine in the dark during the incubations.

4.2. Relevance of pelagic CH₄ production compared to methanotrophy and CH₄ emissions at ecosystem scale

The stable isotope labelling experiments revealed that microbial CH₄ oxidation largely exceed the pelagic CH₄
385 production. All of the major sources and sinks of CH₄ at ecosystem scale were experimentally determined offshore in three
lakes (L. Edward at 20 m depth, George at 2.5 m and Nyamusingere at 3 m) (Fig. 6). In contrast with high latitude lakes where
no ebullition could be detected in location with water column depth higher than 2 m (DelSontro et al. 2018), we found that the
CH₄ ebullition flux dominates over the CH₄ diffusion flux in every sampling site. However, due to the dissolution of arising
bubbles the contribution of ebullition to the total CH₄ emissions might be lower in deeper (> 20 m) location of L. Edward
390 (maximum depth of 113m), as shown elsewhere (DelSontro et al. 2015). Comparison of the CH₄ production, consumption and
emission fluxes (Fig 6.) show that the, depth-integrated CH₄ production rates determined from diverse precursors molecules
were modest relative to the diffusive CH₄ efflux to the atmosphere and the depth-integrated microbial CH₄ oxidation.. In
opposition, the combined CH₄ bubble dissolution flux and diffusive benthic CH₄ flux were several orders of magnitude higher
than CH₄ production in surface waters, and were sufficient to support the microbial CH₄ oxidation and the emissions to the
395 atmosphere (Fig. 6). These results gathered in tropical lakes of various size (from 0.44 to 2300 km²) and depth are in sharp
contrast with the estimation of an empirical model (Gunthel et al. 2019) which proposed that mechanisms of oxic CH₄
production represents the majority of CH₄ emissions in lakes larger than 1 km². This discrepancy highlights the need to consider
the unique limnological characteristics of a vast region of the world that harbours 16% of the total surface of lakes (Lehner &
Doll 2004). One of the most distinctive features of tropical aquatic environment is the persistent elevated water temperature in
400 the hypolimnion and at the water-sediment interface which favours methanogenic activity in sediment and decreases CH₄
solubility, enhancing bubbles formation.

Epilimnetic CH₄ production appeared as a marginal flux at the ecosystem scale and could not explain alone the
accumulation of ¹³C-depleted CH₄ in the epilimnion of most of the lakes of our dataset (Figs. 1, 2), for which we propose a
combination of two other alternative mechanisms: dissolution of arising CH₄ bubbles in the epilimnion combined with
405 inhibition by light of CH₄ oxidation. The partial dissolution of the CH₄ bubbles as they rise in the epilimnion would allow a
rapid transport of ¹³C-depleted CH₄ from the sediment, bypassing the hotspot of CH₄ oxidation at the sediment-water interface
and representing an alternative source of ¹³C-depleted CH₄ in water column. This mechanism of bubble-mediated transport to
the epilimnion would be especially important in shallow lakes as CH₄ ebullition is widely variable in function of water column
depth (DelSontro et al. 2015). The shallower L. George and L. Nyamusingere were notably characterized by sharp thermal
410 density gradients (Fig. 2) and extreme phytoplankton biomass largely dominated by *Microcystis aeruginosa* (Chlorophyll *a* up

to 190 $\mu\text{g L}^{-1}$). *Microcystis aeruginosa* cells form large aggregates (>1 mm) embedded in a matrix of extracellular polymeric substance that might act as a barrier to trap small CH_4 bubbles arising from the sediment (Fig S7). Dissolution of CH_4 bubbles could be enhanced at the very near surface due to the entrapments of bubbles at the air-water interface by abundant surface organic films that delay the bubble “burst”. The presence of a sharp sub-surface temperature gradient would further enhance
415 CH_4 accumulation during day-time near the air-water interface (by blocking vertical redistribution of CH_4 by mixing). We hypothesize that this process could be widespread in shallow tropical lakes which are characterized by high productivity and are susceptible to be simultaneous large benthic CH_4 sources.

The stable isotope labelling experiment carried out to investigate the inhibitory effect of light on methanotrophic activity demonstrated that CH_4 consumption dramatically decreased with increasing light intensities (Fig. 5), as already
420 reported in a tropical reservoir (Dumestre et al. 1999) and Lake Biwa (Murase et al. 2005). The inhibitory effect of light on freshwater methanotrophs remains surprisingly understudied since it was first reported 20 years ago (Dumestre et al. 1999), so that the physiological mechanism of photoinhibition is still not understood. The physiological mechanism of photoinhibition of CH_4 oxidation could be related to the fact that the copper-containing methane monooxygenase enzyme and structurally close to the ammonia monooxygenase enzyme, and might be inactivated by ROS produced during photooxidative stress, as
425 shown for ammonium oxidizers (French et al. 2012, Tolar et al. 2016). Altogether, our results emphasize the role of sunlight irradiance as an important, but frequently overlooked, environmental factor driving the CH_4 dynamics in lake surface waters and possibly contributing to the occurrence of ^{13}C depleted CH_4 in surface waters.

5. Supplement

Supplementary figures are available on-line on the *Biogeosciences* website.

430 6. Data availability

All data included in this study are available upon request by contacting the corresponding author.

7. Author contributions

This study was designed by C. Morana, A.V. Borges & S. Bouillon. All authors participated to samples collection, data acquisition and analysis. The manuscript was drafted by C. Morana and substantially improved with the inputs of all authors.
435 All authors approved the final version of the manuscript.

8. Competing interests

The authors declare that they have no conflict of interest.

9. Acknowledgments

We are grateful to Marc-Vincent Commarieu and Dries Grauwels for their help in the lab and during the field sampling. We
440 also thank the Uganda Wildlife Agency for research permission in the Queen Elizabeth National Park (Uganda), the staff of the Tembo Canteen for the use of their incubation room and the crew of the Katwe Marine Research Vessel for their help during the L. Edward sampling. We also thank the associate editor (Dr. Tyler Cyronak) and two anonymous reviewers who helped to improve the initial version of this manuscript. This work was funded by the Belgian Federal Science Policy Office (BELSPO, HIPE project, BR/154/A1/HIPE) and by the Fonds Wetenschappelijk Onderzoek (FWO-Vlaanderen, Belgium)
445 with travel grants awarded to CM and SB. AVB is a research director at the Fond National de la Recherche Scientifique (FNRS, Belgium).

10. References

Bastviken, D., Ejlertsson, J., Sundh, I., & Tranvik, L.: Methane as a source of carbon and energy for lake pelagic food webs. *Ecology*, 84(4), 969-981, 2003

- 450 Bastviken, D., Tranvik, L. J., Downing, J. A., Crill, P. M., & Enrich-Prast, A.: Freshwater methane emissions offset the continental carbon sink, *Science*, 331(6013), 50-50, 2011
- Baines, S. B., & Pace, M. L.: The production of dissolved organic matter by phytoplankton and its importance to bacteria: patterns across marine and freshwater systems. *Limnology and Oceanography*, 36(6), 1078-1090, doi: 10.4319/lo.1991.36.6.1078, 1991
- 455 Bishop, N. I.: The influence of the herbicide, DCMU, on the oxygen-evolving system of photosynthesis. *Biochimica et biophysica acta*, 27(1), 205-206, doi: 10.1016/0006-3002(58)90313-5, 1958
- Bižić, M., Ionescu, D., Günthel, M., Tang, K. W., & Grossart, H. P.: Oxidic Methane Cycling: New Evidence for Methane Formation in Oxidic Lake Water. *Biogenesis of Hydrocarbons*, 1-22, 2018
- Bižić, M., Klintzsch, T., Ionescu, D., Hindiyeh, M. Y., Günthel, M., Muro-Pastor, A. M., Eckert, W., Urich, T., & 460 Grossart, H. P.: Aquatic and terrestrial cyanobacteria produce methane. *Science advances*, 6(3), eaax5343, doi: 10.1126/sciadv.aax5343, 2020
- Bogard, M. J., Del Giorgio, P. A., Boutet, L., Chaves, M. C. G., Prairie, Y. T., Merante, A., & Derry, A. M.: Oxidic water column methanogenesis as a major component of aquatic CH₄ fluxes. *Nature communications*, 5, 5350, doi: 10.1038/ncomms6350, 2014
- 465 Borges, A. V., Darchambeau, F., Teodoru, C. R., Marwick, T. R., Tamooh, F., Geeraert, N., Morana, C., Okuku, E. & Bouillon, S.: Globally significant greenhouse-gas emissions from African inland waters. *Nature Geoscience*, 8(8), 637-642, 2015
- Bruhn, D., Möller, I. M., Mikkelsen, T. N., & Ambus, P.: Terrestrial plant methane production and emission. *Physiologia plantarum*, 144(3), 201-209, doi: 10.1111/j.1399-3054.2011.01551, 2012
- 470 Cole, J. J., & Caraco, N. F.: Atmospheric exchange of carbon dioxide in a low-wind oligotrophic lake measured by the addition of SF₆. *Limnology and Oceanography*, 43(4), 647-656, doi: 10.4319/lo.1998.43.4.0647, 1998
- Damm, E., Helmke, E., Thoms, S., Schauer, U., Nöthig, E., Bakker, K., & Kiene, R. P.: Methane production in aerobic oligotrophic surface water in the central Arctic Ocean. *Biogeosciences*, 7(3), 1099-1108, doi: 10.5194/bg-7-1099-2010, 2010
- 475 DelSontro, T., McGinnis, D. F., Wehrli, B., and Ostrovsky, I.: Size does matter: Importance of large bubbles and small-scale hot spots for methane transport. *Environmental science & technology*, doi.org/10.1021/es5054286, 2015
- DelSontro, T., del Giorgio, P. A., & Prairie, Y. T.: No longer a paradox: the interaction between physical transport and biological processes explains the spatial distribution of surface water methane within and across lakes. *Ecosystems*, 21(6), 1073-1087, doi: 10.1007/s10021-017-0205-1, 2018
- 480 Delwiche, K. B., and Hemond, H. F.: Methane bubble size distributions, flux, and dissolution in a freshwater lake. *Environmental Science & Technology*, doi.org/10.1021/acs.est.7b04243, 2017
- Denman, S. E., Tomkins, N. W., & McSweeney, C. S.: Quantitation and diversity analysis of ruminal methanogenic populations in response to the antimethanogenic compound bromochloromethane. *FEMS microbiology ecology*, 62(3), 313-322, doi: 10.1111/j.1574-6941.2007.00394.x, 2007
- 485 Descy, J. P., Darchambeau, F., Lambert, T., Stoyneva-Gaertner, M. P., Bouillon, S., & Borges, A. V.: Phytoplankton dynamics in the Congo River. *Freshwater Biology*, 62(1), 87-101, doi: 10.1111/fwb.1285, 2017
- Donis, D., Flury, S., Stöckli, A., Spangenberg, J. E., Vachon, D., & McGinnis, D. F. (2017). Full-scale evaluation of methane production under oxidic conditions in a mesotrophic lake. *Nature communications*, 8(1), 1661, doi: 10.1038/s41467-017-01648-4, 2017
- 490 Dumestre, J. F., Guézennec, J., Galy-Lacaux, C., Delmas, R., Richard, S., and Labroue, L.: Influence of light intensity on methanotrophic bacterial activity in Petit Saut Reservoir, French Guiana. *Applied and environmental microbiology*, doi: 10.1128/AEM.65.2.534-539, 1999

- Fernández, J. E., Peeters, F., & Hofmann, H.: On the methane paradox: Transport from shallow water zones rather than in situ methanogenesis is the major source of CH₄ in the open surface water of lakes. *Journal of Geophysical Research: Biogeosciences*, 121(10), 2717-2726, doi: 10.1002/2016JG003586, 2016
- 495 French, E., Kozłowski, J. A., Mukherjee, M., Bullerjahn, G., & Bollmann, A.: Ecophysiological characterization of ammonia-oxidizing archaea and bacteria from freshwater. *Applied and Environmental Microbiology*, 78(16), 5773-5780, doi: 10.1128/aem.00432-12, 2012
- Gillikin, D. P., and Bouillon, S.: Determination of delta O-18 of water and delta C-13 of dissolved inorganic carbon using a simple modification of an elemental analyzer-isotope ratio mass spectrometer: an evaluation. *Rapid Communications in Mass Spectrometry*, doi: 10.1002/rcm.2968, 2007
- 500 Greinert, J. and McGinnis, D.F.: Single Bubble Dissolution Model: The Graphical User Interface SiBu-GUI. *Environmental Modelling & Software*, doi:10.1016/j.envsoft.2008.12.011, 2009
- Grossart, H. P., Frindte, K., Dziallas, C., Eckert, W., & Tang, K. W.: Microbial methane production in oxygenated water column of an oligotrophic lake. *Proceedings of the National Academy of Sciences*, 108(49), 19657-19661, doi: 10.1073/pnas.1110716108, 2011
- 505 Günthel, M., Donis, D., Kirillin, G., Ionescu, D., Bizic, M., McGinnis, D. F., Grossart, H. P., & Tang, K. W.: Contribution of oxic methane production to surface methane emission in lakes and its global importance. *Nature communications*, 10(1), doi: 10.1038/s41467-019-13320-0, 2019
- Hama, T., Miyazaki, T., Ogawa, Y., Iwakuma, T., Takahashi, M., Otsuki, A., & Ichimura, S.: Measurement of photosynthetic production of a marine phytoplankton population using a stable ¹³C isotope. *Marine Biology*, 73(1), 31-36, doi: 10.1007/BF00396282, 1983
- 510 Hofmann, H., Federwisch, L., & Peeters, F.: Wave-induced release of methane: littoral zones as source of methane in lakes. *Limnology and Oceanography*, 55(5), 1990-2000, doi: 10.4319/lo.2010.55.5.1990 2010
- Klindworth, A., Pruesse, E., Schweer, T., Peplies, J., Quast, C., Horn, M., & Glöckner, F. O.: Evaluation of general 16S ribosomal RNA gene PCR primers for classical and next-generation sequencing-based diversity studies. *Nucleic acids research*, 41(1), doi: 10.1093/nar/gks808, 2013
- 515 Klintzsch, T., Langer, G., Nehrke, G., Wieland, A., Lenhart, K., & Keppler, F.: Methane production by three widespread marine phytoplankton species: release rates, precursor compounds, and potential relevance for the environment. *Biogeosciences*, 16(20), 4129-4144, doi: 10.5194/bg-16-4129-2019, 2019
- 520 Kosten, S., Huszar, V. L., Bécares, E., Costa, L. S., van Donk, E., Hansson, L. A., Jeppesen, E., Kruk, C., Lacerot, G., Mazzeo, N., De Meester, L., Moss, B., Lurling, M., Noges, T., Romo, S., & Scheffer, M.: Warmer climates boost cyanobacterial dominance in shallow lakes. *Global Change Biology*, 18(1), 118-126, doi: 10.1111/j.1365-2486.2011.02488.x, 2012
- Kozich, J. J., Westcott, S. L., Baxter, N. T., Highlander, S. K., & Schloss, P. D.: Development of a dual-index sequencing strategy and curation pipeline for analyzing amplicon sequence data on the MiSeq Illumina sequencing platform. *Applied and environmental microbiology*, AEM-01043, doi: 10.1128/aem.01043-13, 2013
- 525 Lehner, B., Döll, P.: Development and validation of a global database of lakes, reservoirs and wetlands. *Journal of Hydrology*, 296: 1-22, doi: 10.1016/j.jhydrol.2004.03.028, 2004
- Lenhart, K., Klintzsch, T., Langer, G., Nehrke, G., Bunge, M., Schnell, S., & Keppler, F.: Evidence for methane production by the marine algae *Emiliania huxleyi*. *Biogeosciences*, 13(10), 3163-3174, doi:10.5194/bg-13-3163-2016, 2016
- 530 Levine, R. L., Mosoni, L., Berlett, B. S., & Stadtman, E. R.: Methionine residues as endogenous antioxidants in proteins. *Proceedings of the National Academy of Sciences*, 93(26), 15036-15040, doi: 10.1073/pnas.93.26.15036, 1996
- Lewis Jr, W. M.: Tropical limnology. *Annual review of ecology and systematics*, 18(1), 159-184, doi: 10.1146/annurev.es.18.110187.001111, 1987

- 535 Martinez-Cruz, K., Sepulveda-Jauregui, A., Greene, S., Fuchs, A., Rodriguez, M., Pansch, N., Gonsiorczyk, T., & Casper, P.: Diel variation of CH₄ and CO₂ dynamics in two contrasting temperate lakes. *Inland Waters*, 1-15, doi: 10.1080/20442041.2020.1728178, 2020
- McGinnis, D. F., Greinert, J., Artemov, Y., Beaubien, S. E., & Wüest, A. N. D. A.: Fate of rising methane bubbles in stratified waters: How much methane reaches the atmosphere?. *Journal of Geophysical Research: Oceans*, 111(C9), doi: 10.1029/2005JC003183, 2006
- 540 Mohr, W., Grosskopf, T., Wallace, D. W., & LaRoche, J.: Methodological underestimation of oceanic nitrogen fixation rates. *PloS one*, 5(9), e12583, doi: 10.1371/journal.pone.0012583, 2010
- Montoya, J. P., Voss, M., Kahler, P., & Capone, D. G.: A Simple, High-Precision, High-Sensitivity Tracer Assay for N (inf2) Fixation. *Appl. Environ. Microbiol.*, 62(3), 986-993. doi: 10.1128/aem.62.3.986-993.1996, 1996
- 545 Morana, C., Borges, A. V., Roland, F. A. E., Darchambeau, F., Descy, J. P., & Bouillon, S.: Methanotrophy within the water column of a large meromictic tropical lake (Lake Kivu, East Africa). *Biogeosciences*, 12(7), 2077-2088, doi: 10.5194/bg-12-2077-2015, 2015
- Mountfort, D. O. & Asher, R. A. Effect of inorganic sulfide on the growth and metabolism of *Methanosarcina barkeri* strain DM. *Appl. Environ. Microbiol.* 37, 670–675 (1979).
- 550 Morana, C., Sarmiento, H., Descy, J. P., Gasol, J. M., Borges, A. V., Bouillon, S., & Darchambeau, F.: Production of dissolved organic matter by phytoplankton and its uptake by heterotrophic prokaryotes in large tropical lakes. *Limnology and Oceanography*, 59(4), 1364-1375. doi:10.4319/lo.2014.59.4.1364, 2014
- Morana, C., Darchambeau, F., Roland, F., Borges, A., Muvundja, F., Kelemen, Z., Masilya, P., Descy J-P., and Bouillon, S.: Biogeochemistry of a large and deep tropical lake (Lake Kivu, East Africa: insights from a stable isotope study covering an annual cycle. *Biogeosciences*, doi:10.5194/bg-12-4953-2015, 2015
- 555 Mugidde, R., Hecky, R. E., Hendzel, L. L., & Taylor, W. D.: Pelagic nitrogen fixation in lake Victoria (East Africa). *Journal of Great Lakes Research*, 29, 76-88, doi: 10.1016/S0380-1330(03)70540-1, 2003
- Murase, J., & Sugimoto, A: Inhibitory effect of light on methane oxidation in the pelagic water column of a mesotrophic lake (Lake Biwa, Japan). *Limnology and oceanography*, 50(4), 1339-1343, doi: doi.org/10.4319/lo.2005.50.4.1339, 2005
- 560 Peeters, F., Fernandez, J. E., & Hofmann, H.: Sediment fluxes rather than oxic methanogenesis explain diffusive CH₄ emissions from lakes and reservoirs. *Scientific reports*, 9(1), 1-10, doi: doi.org/10.1038/s41598-018-36530-w, 2019
- Petrillo, E., Herz, M. A. G., Fuchs, A., Reifer, D., Fuller, J., Yanovsky, M. J., Simpson, C., Brown, J. W. S., Barta, A., Kalyna, M., & Kornblihtt, A. R.: A chloroplast retrograde signal regulates nuclear alternative splicing. *Science*, 344(6182), 427-430, doi: 10.1126/science.1250322, 2014
- 565 Repine, J. E., Eaton, J. W., Anders, M. W., Hoidal, J. R., & Fox, R. B.: Generation of hydroxyl radical by enzymes, chemicals, and human phagocytes in vitro: detection with the anti-inflammatory agent, dimethyl sulfoxide. *The Journal of clinical investigation*, 64(6), 1642-1651, doi: 10.1172/jci109626, 1979
- Sarmiento, H., Romera-Castillo, C., Lindh, M., Pinhassi, J., Sala, M. M., Gasol, J. M., Marassé, C., & Taylor, G. T.: Phytoplankton species-specific release of dissolved free amino acids and their selective consumption by bacteria. *Limnology and Oceanography*, 58(3), 1123-1135, doi: 10.4319/lo.2013.58.3.1123, 2013
- 570 Tang, K. W., McGinnis, D. F., Ionescu, D., & Grossart, H. P.: Methane production in oxic lake waters potentially increases aquatic methane flux to air. *Environmental science & technology Letters*, 3(6), 227-233, doi: 10.1021/acs.estlett.6b00150, 2016
- 575 Tolar, B. B., Powers, L. C., Miller, W. L., Wallsgrove, N. J., Popp, B. N., & Hollibaugh, J. T.: Ammonia oxidation in the ocean can be inhibited by nanomolar concentrations of hydrogen peroxide. *Frontiers in Marine Science*, 3, 237, doi: 10.3389/fmars.2016.00237, 2016

Vollenweider R.A.: Calculations models of photosynthesis-depth curves and some implications regarding day rate estimates in primary production measurements. *Memorie dell'Istituto Italiano di Idrobiologia*, 18, 425–457, 1965

580 Wanninkhof, R.: Relationship between wind speed and gas exchange over the ocean. *Journal of Geophysical Research: Oceans*, 97(C5), 7373-7382, doi: 10.1029/92JC00188, 1992

Yao, M., Henny, C., & Maresca, J. A.: Freshwater bacteria release methane as a byproduct of phosphorus acquisition. *Applied and environmental microbiology*, 82(23) 6994-7003, doi: 10.1128/aem.02399-16, 2016

585 Yvon-Durocher, G., Allen, A. P., Bastviken, D., Conrad, R., Gudasz, C., St-Pierre, A., Thanh-Duc, N., & Del Giorgio, P. A.: Methane fluxes show consistent temperature dependence across microbial to ecosystem scales. *Nature*, 507, 488-491, doi: 10.1038/nature13164, 2014

590

595

600

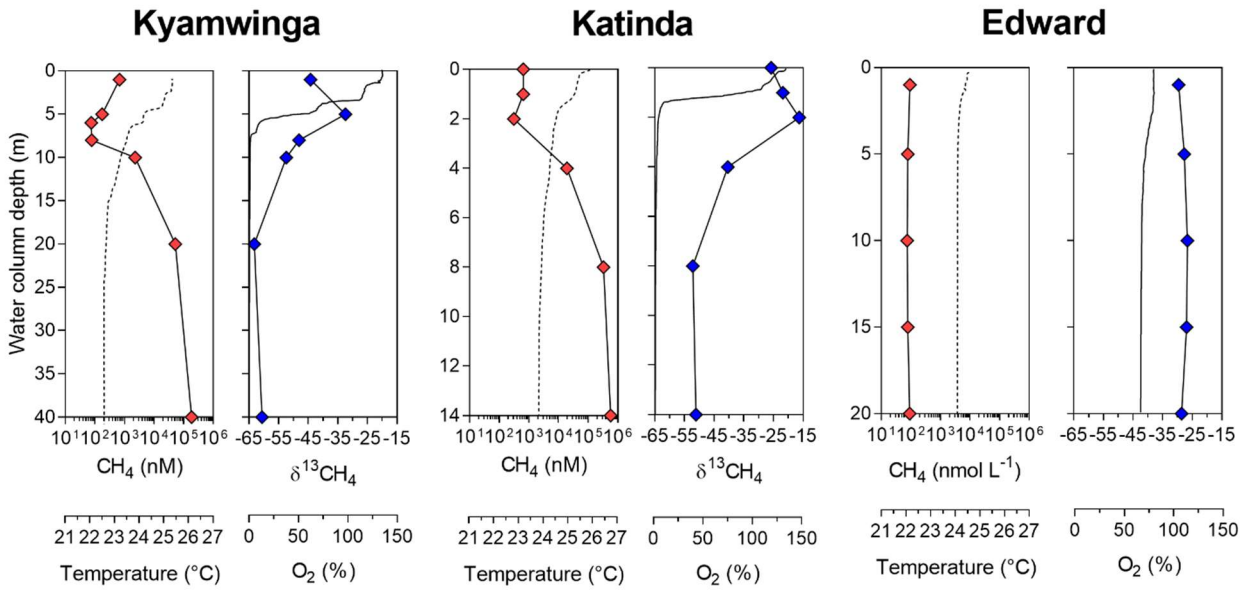
605

610

615

620

11. Figure captions



625

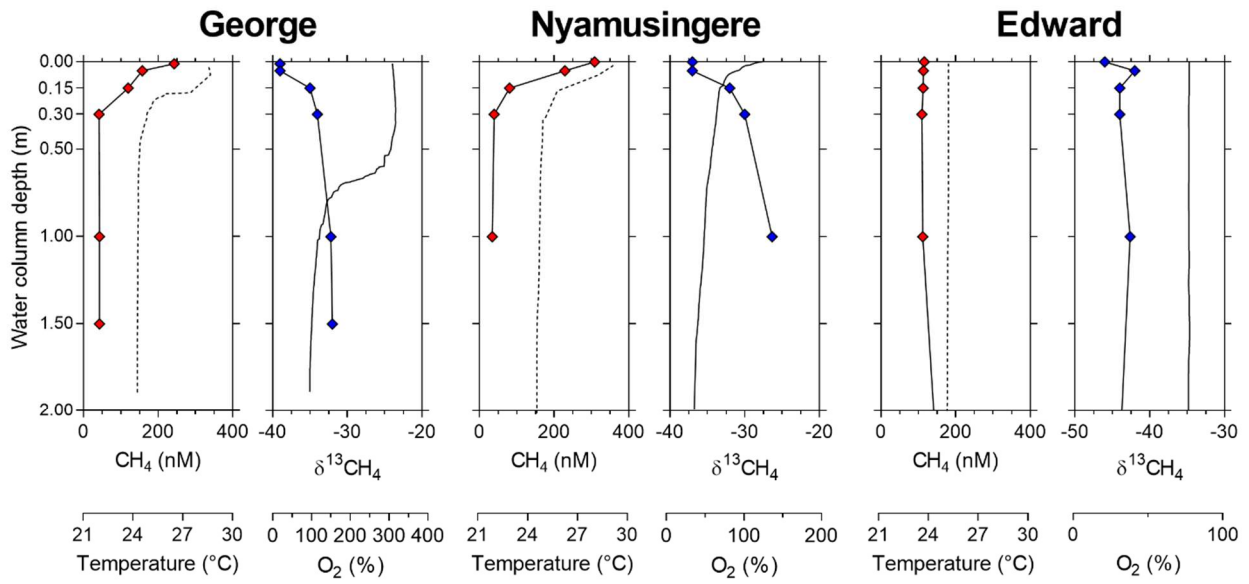
Figure 1. Depth profile. Depth profile of the temperature (°C ; dashed line), CH₄ concentration (nmol L⁻¹ ; red symbols), dissolved oxygen saturation (% , solid line) and stable isotope carbon composition of CH₄ (δ¹³C-CH₄, ‰ ; blue symbols) in Lake Kyamwinda (left), Lake Katinda (middle), and Lake Edward (right).

630

635

640

645



650 **Figure 2. Depth profile, focus on the surface.** Depth profile of the temperature (°C ; dashed line), CH₄ concentration (nmol L⁻¹ ; red symbols), dissolved oxygen saturation (% , solid line) and stable isotope carbon composition of CH₄ (δ¹³C-CH₄, ‰ ; blue symbols) in Lake George (left), Lake Nyamusingere (middle), and the surface waters (0-2 m) of Lake Edward (right).

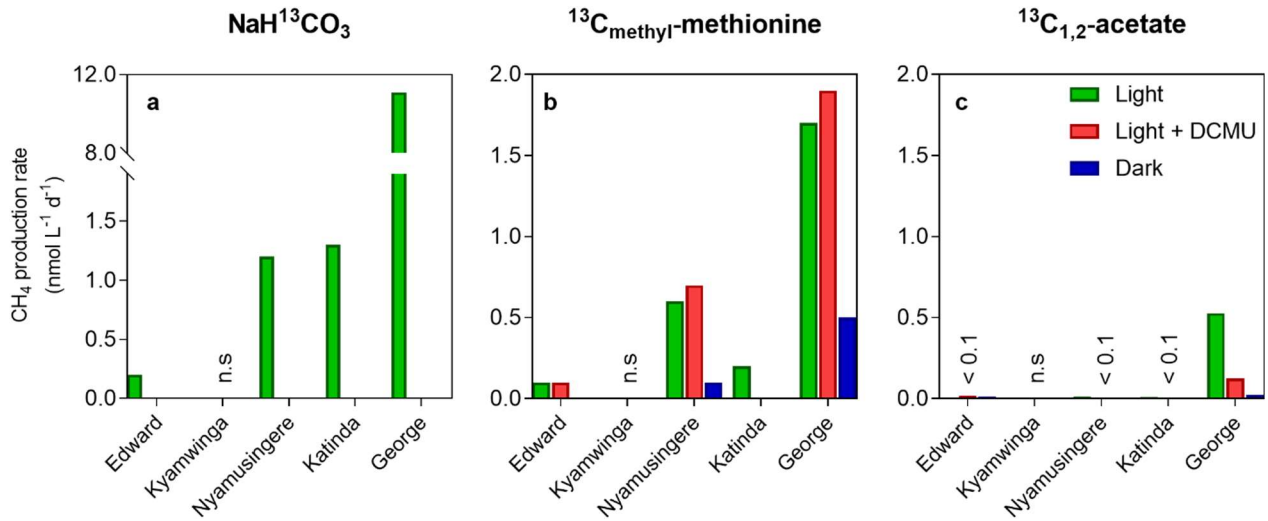
655

660

665

670

675



680

Figure 3. Tracer experiments show CH₄ production in well-oxygenated surface waters. CH₄ production rates (nmol L⁻¹ d⁻¹) from dissolved inorganic carbon (a), the methyl group of methionine (b) and acetate (c) measured in the surface waters (0.3 m) of a variety of African tropical lakes. Green, grey and dark bars respectively represent rates measured under light, light in presence of a photosynthesis inhibitor (DCMU), or darkness. Values showed for L. Edward, L. George and L. Katinda are the average of 2017 and 2018 sampling campaign measurement. n.s = not significant, < 0.1 = below 0.1 nmol L⁻¹ d⁻¹.

685

690

695

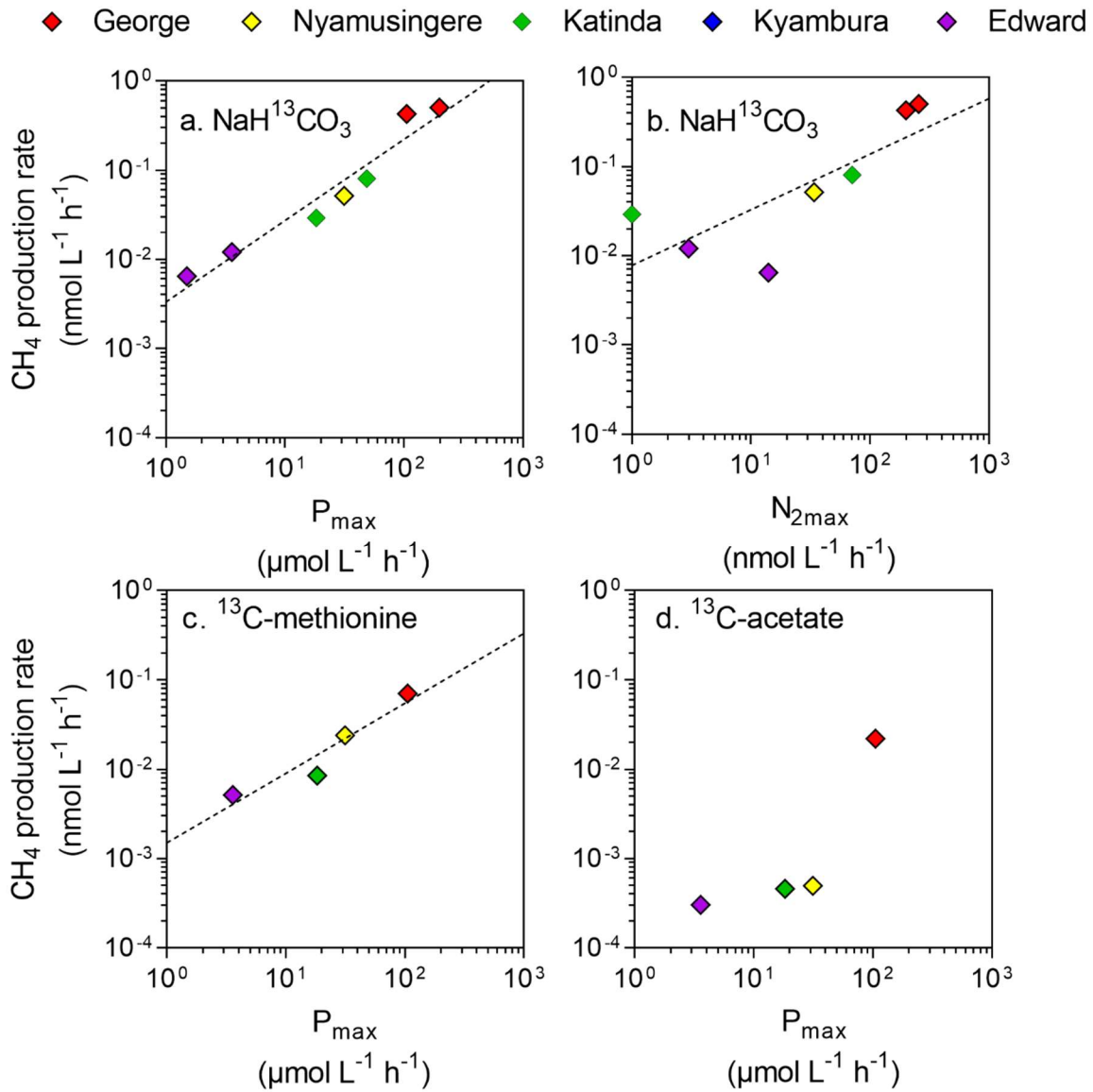


Figure 4. Direct link between CH₄ production and phytoplankton metabolism. Relationship between the maximum photosynthetic activity (P_{max} , μmol C L⁻¹ h⁻¹) or maximum nitrogen fixation rates (N_{2max} , nmol L⁻¹ h⁻¹) and surface CH₄ production rates (nmol C L⁻¹ h⁻¹) from dissolved inorganic carbon (a, b), methyl group of methionine (c), and acetate (d).

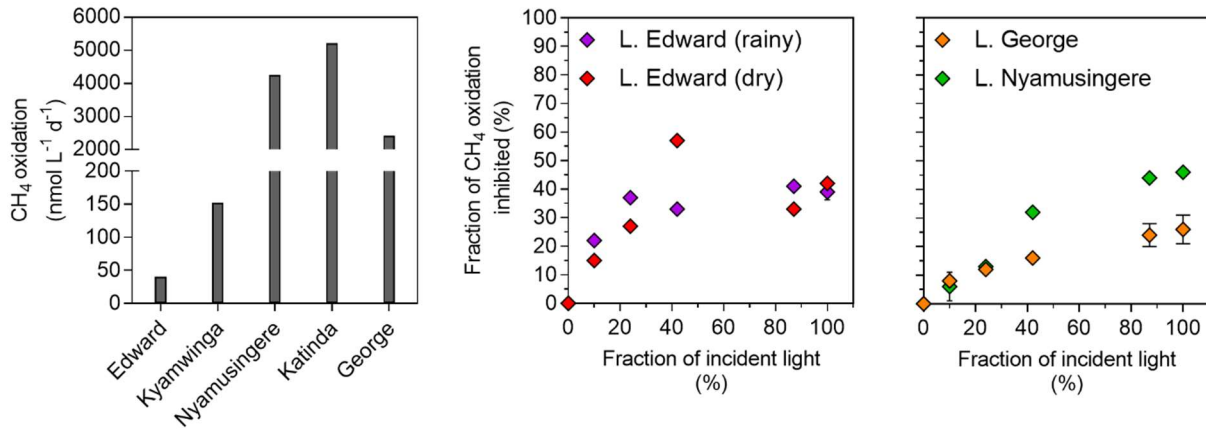


Figure 5. Light inhibition patterns of CH₄ oxidation in surface waters. Left panel: CH₄ oxidation rates (nmol L⁻¹ d⁻¹) measured in the surface waters (0.3 m) in the dark of a variety of African tropical lakes. Right panel: relationship between illumination (fraction of incident sunlight irradiance, %) and CH₄ oxidation inhibition (fraction of CH₄ oxidation in the dark inhibited at a given irradiance, %) in Lake Edward, Lake George and Lake Nymusingere. Symbols represent the mean, and error bars represent the maximum and minimum of duplicate experiments

720

725

730

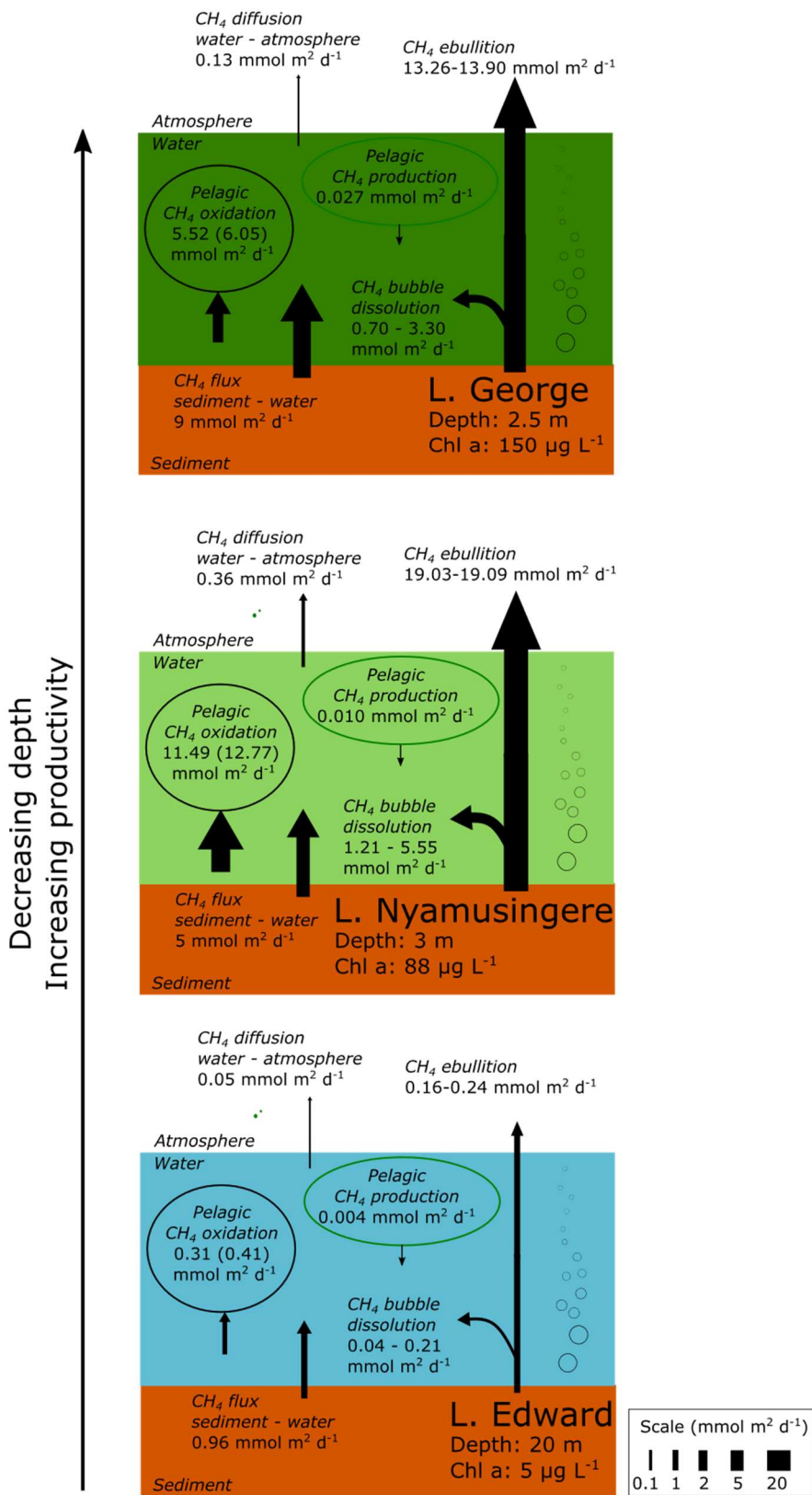


Figure 6. Epilimnetic CH₄ production is a marginal source of CH₄ compared to sedimentary sources and CH₄ sinks in several contrasting African lakes. Summary of the different CH₄ flux experimentally measured in L. Edward, L. George and L. Nyamusingere. Values of CH₄ oxidation in brackets are values not considering CH₄ photoinhibition. Pelagic CH₄ production are values determined from NaH¹³CO₃ (~5% final enrichment) and ¹³C-acetate (99% final enrichment), as described in the methods section. ¹³C-labelling experiment carried out under constant light irradiance. CH₄ flux at the water-air and sediment-water interface were determined experimentally as described in the Methods. CH₄ bubble dissolution and CH₄ ebullition flux were determined using the SiBu-GUI software (Greinert & McGinnis 2009); minimum and maximum represents the values obtained from two extreme bubble-size scenarios considering a release of many small (3 mm diameter) bubbles or fewer large (10 mm) bubbles.